34th Annual International Conference of the IEEE EMBS
San Diego, California USA, 28 August - 1 September, 2012

Roles of Bioactive Sphingolipid Metabolites in Ovarian Cancer Cell Biomechanics*

Hesam Babahosseini, Paul C. Roberts, Eva M. Schmelz, and Masoud Agah, *Senior Member, IEEE*

Abstract— **Bioactive Sphingolipid metabolites have emerged as important lipid second messengers in the regulation of cell growth, death, motility and many other events. These processes are important in cancer development and progression; thus, sphingolipid metabolites have been implicated in both cancer development and cancer prevention. Despite recent considerable progress in understanding the multi-faceted functions of these bioactive metabolites, little is known about their influence on the biomechanical property of cells. The biomechanical properties of cancer cells change during progression with aggressive and invasive cells being softer compared to their benign counterparts. In this paper, we investigated the effects of exogenous sphingolipid metabolites on the Young's modulus and cytoskeletal organization of cells representing aggressive ovarian cancer. Our findings demonstrate that the elasticity of aggressive ovarian cancer cells decreased ~15% after treatment with ceramide and sphingosine-1-phosphate. In contrast, sphingosine treatment caused a ~30% increase in the average elasticity which was associated with a more defined actin cytoskeleton organization. This indicates that sphingolipid metabolites differentially modulate the biomechanic properties of cancer cells which may have a critical impact on cancer cell survival and progression, and the use of sphingolipid metabolites as chemopreventive or chemo-therapeutic agents.**

I. Introduction

Bioactive sphingolipid metabolites such as ceramide (Cer), sphingosine (So), and sphingosine-1-phosphate (S1P) play crucial roles in cell growth, differentiation, death, motility and many other cellular processes [1, 2]. While Cer and So in general mediate anti-proliferative and cytotoxic responses [1] and suppress cancer cell growth *in vitro* and *in vivo* [3, 4], S1P often induces cell growth, survival, motility and angiogenesis, supporting tumor development and progression [5, 6]. These metabolites are easily inter-convertible; in response to growth factors, inflammatory stimuli, stresses and other stimuli, cells generate a distinct sphingolipid metabolite profile to mediate the cellular response. This is dependent among other factors on the accumulating sphingolipid species, their concentrations, exposure time, intracellular localization and the targeted tissue.

Sphingolipid metabolites modulate the cytoskeleton organization in various tissues. Cer has been shown to induce stress fibers in fibroblast [7] while S1P plays a role in the rearrangement of the cytoskeleton in endothelial cells [8]. The effects of these metabolites on ovarian cancer cells are not known.

In mouse ovarian surface epithelial (MOSE) cells, a cell model for progressive ovarian cancer, changes in cell morphology and tumorigenicity during progression [9] were accompanied by changes in genes encoding cytoskeleton proteins and their regulators and an increasingly disorganized actin cytoskeleton [10]. The deformability and the cytoskeleton organization of the MOSE cells correlate with their malignant state; accordingly, the cells become softer and less viscous as they progress toward more aggressive stages [11], confirming our previous studies in breast cancer models and many other studies [12-15]. Subsequent studies identified the actin cytoskeleton as a critical contributor in defining cell's viscoelastic properties [16].

The present paper investigates the effects of Cer, S1P, and So on the elasticity of aggressive MOSE cells to determine if these bioactive metabolites can reverse changes in the biomechanical properties established during cancer progression. For these studies we utilized atomic force microscopy (AFM) in conjunction with the Hertz contact model. Our results demonstrate the differential responses of the MOSE cells to the treatments, aiding our understanding of the sphingolipids metabolites functions which could be utilized for the development of novel sphingolipid-based therapeutic strategies against ovarian and potentially other cancers.

II. Cell Culturing and Sample Preparation

MOSE cells are a unique murine cell model for progressive ovarian cancer, generated from mouse ovarian surface epithelial cells as described [9]. According to their genotype and phenotype, they are categorized into early/benign, intermediate, and late/aggressive. MOSE cells are maintained in High Glucose Dulbecco's Modified Eagle's Medium containing 40 mL/L (4%) Fetal Bovine Serum, 3.7 g/L of Sodium Bicarbonate and 10 mL/L of Insulin-Transferin-Selenium, and 10 mL/L (1%) of a Penicillin-Streptomycin solution. Cells were grown at 37°C in a humidified 5% CO_2 atmosphere. Parallel cultures were

*Research supported by the ICTAS, the NSF Foundation, and NIH R01 CA 118846 (to EMS and PCR).

H. Babahosseini is with VT MEMS Lab, Department of Mechanical Engineering, Virginia Tech, Blacksburg, VA, USA (e-mail: hbabahosseini@vt.edu).

P. C. Roberts is with the Department of Biomedical Sciences and Pathobiology, Virginia Tech, Blacksburg, VA, USA (e-mail: pcroberts@vt.edu).

E. M. Schmelz is with the Department of Human Nutrition, Foods and Exercise, Virginia Tech, Blacksburg, VA, USA (e-mail: eschmelz@vt.edu).

M. Agah is with VT MEMS Lab, the Bradley Department of Electrical and Computer Engineering, Virginia Tech, Blacksburg, VA, USA (corresponding author; phone: 504-231-2653; fax: 540-231-3362; e-mail: agah@vt.edu).

treated with 2 μM Cer, 500 nM S1P, and 1.5 μM So for at least three passages. These concentrations of sphingolipid metabolites were not toxic for the cells. For AFM sample preparation, the cells were plated at a density of 3×10^4 cells/mm^2 on 25 mm glass cover slips and incubated for 24 hr prior to the experiments. The density of the cells was selected so to have a sufficient number of single cells during the AFM experiment. Cover slips were coated with 0.1 mg/mL collagen type IV (Sigma) for 24 hr to allow cells to attach to the substrate.

III. Atomic Force Microscopy

All the AFM measurements were performed using a Multimode V SPM (Veeco Instruments, Santa Barbara, CA, USA). V-shaped SiNi cantilevers, TR400PSA (Olympus, Tokyo, Japan) with a nominal spring constant of 0.02 N/m were used. To reduce the stress on the cells which can damage the soft samples and to remove any nonlinearity in deforming stress, the cantilever tip should be altered to increase the total surface contact area. For this purpose, a glass microsphere (Duke Scientific, Palo Alto, California) with an approximate diameter of ~10 μm was attached to the cantilever tip. Since all measurements are supposed to correspond to the cell nuclei region, increasing the contact surface guarantees that the center of cells is indented.

All the elasticity measurements were carried out at room temperature. Since the cell elastic modulus depends on the indentation speed, the tip approach velocity was kept at ~0.5 μm/s during the measurements and data were acquired at a sample rate of 5 kHz. Moreover, all the force-distance curves were obtained with a maximum force trigger of 1.5±0.3 nN.

IV. Hertz Model and Data Analysis

Several contact mechanics models such as DMT, JKR, and Hertz models have been developed for describing contact deformations. An extended version of the Hertz model which is appropriate for deformation of soft materials like biological cells is used here to extract elastic modulus of the cells [17]. According to the model, in interaction between a spherical tip and a sample cell, the relationship between the applied force, F and the induced indentation depth, δ can be expressed as:

$$F = \frac{4}{3} E^* \sqrt{R}.\delta^{\frac{3}{2}} \quad (1)$$

where R is the radius of the spherical glass bead attached on the tip and E^* is the equivalent elastic modulus of two contact surfaces. For the extremely hard tip in comparison to the sample, $E^* = E_{cell} / (1-\nu_{cell}^2)$, where E is the Young's modulus and ν is the Poisson's ratio of the cell. The Poisson's ratio is assumed to be 0.5 assuming biological cells are incompressible [18]. The indentation depth can be calculated as the difference in the relative movement of the piezo scanner and deflection of the cantilever as the following:

$$\delta = (z - z_0) - (d - d_0) \quad (2)$$

where z_0 and d_0 are the piezo scanner position and the cantilever deflection at the initial contact point between the tip and the cell sample. There is a big issue to find the coordination of the initial contact point and fit the most appropriate region of the acquired data to the Hertz model. Simply, the difficulty can be removed by linearization of (1) in respect to the deformation, δ [19]. By substitution of (2), the Hertz model equation takes the following form:

$$F^{\frac{2}{3}} = \left[\frac{4\sqrt{R}}{3(1-\nu_{cell}^2)}\right]^{\frac{2}{3}} (z-d) - \left[\frac{4\sqrt{R}}{3(1-\nu_{cell}^2)}\right]^{\frac{2}{3}} (z_0 - d_0) \quad (3)$$

Now, the Young's modulus and the contact point's coordination can be computed using the slope and the intercept of the ($F^{2/3}$, z-d) curve. All the analysis including contact point identification, curve fitting of the Hertz model to the collected deflection vs. piezo position raw data were implemented via MATLAB 7.0 software.

V. Results and Discussion

To measure the elastic modulus of the cells, AFM experiments were performed for the control MOSE cells and the sphingolipid metabolites treated cells. Approximately 40-70 single cells were chosen from each population to perform the measurements. The Hertz model was fitted in close proximity to the obtained experimental data with high correlation coefficients of $0.85 \le R^2 \le 0.99$.

The average, standard deviation, and peak values of the measured elastic modulus for all the chosen populations are summarized in Table 1. Treatment of MOSE-L cells with non-toxic concentrations of Cer and S1P caused a downward shift in the average elastic modulus values compared to the control MOSE-L cells. Moreover, there was a decrease in both the standard deviation and the peak value of these populations. The peak values can be extracted by fitting the Gaussian function to the distribution profile of the populations. Conversely, the treatment of MOSE-L cells with So significantly increased the average, standard deviation, and peak value of the measured elastic modulus.

Histograms in Fig. 1 show how Cer, S1P, and So affect the elasticity distribution of the late stage cells. As a result of Cer and S1P treatments, the population distribution shrinks and shifts toward a lower stiffness. However, So treatment causes a notable shift of the distribution toward stiffer values with a broader pattern compared to the control one.

As reported before in [11], When MOSE cells transform from benign to malignant stage, there is a decreasing in the average elasticity and the cells tend to soften. Distributions of elastic modulus also indicated that while benign MOSE cells have a wide distribution, the malignant MOSE cells have a sharp concentration.

TABLE I. ELASTIC BIOMECHANICAL PROPERTIES OF CONTROL LATE STAGE MOSE CELLS AND CER, S1P, AND SO TREATED COUTERPART.

Elasticity (kPa)	***Control MOSE-L***	***Cer treated MOSE-L***	***S1P treated MOSE-L***	***So treated MOSE-L***
mean ± SD	0.847±0.382	0.718±0.298	0.720±0.287	1.085±0.428
peak value	0.746	0.561	0.589	0.859

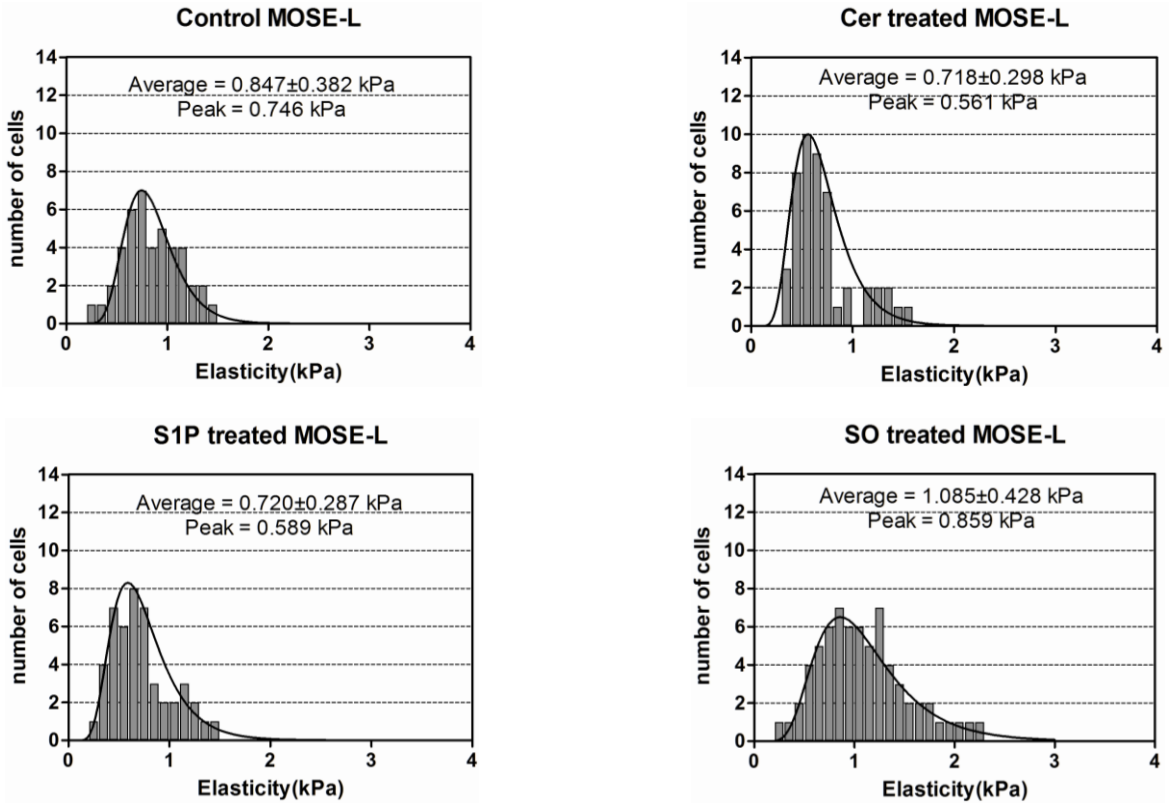

Figure 1. Histograms of control and Cer, S1P, and So treated MOSE-L cells illustrate the effect of the lipids on distribution of measured elastic modulus.

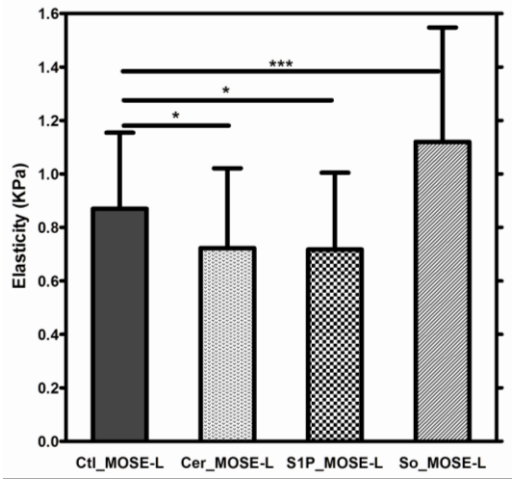

Figure 2. Elastic modulus measurements of MOSE-L cells determine that So treatment significantly increases elasticity ($p \approx 0.0009$) while Cer and S1P treatments decease elasticity ($p \approx 0.01$), all in comparison to the control couterpart.

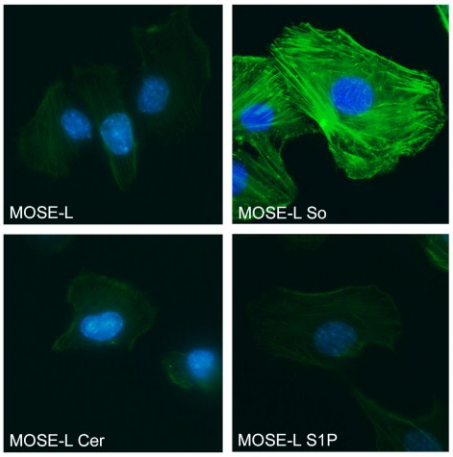

Figure 3. Immunoflurescence images of MOSE-L cells illustrate that So treatment regulates actin fibers organization while Cer and S1P deregulate them. (Note: the images are enhanced to make the actin fibers more visible.)

These observations indicate that So can partially reverse the biomechanical behavior of aggressive MOSE-L cells towards the benign, premalignant precursor cells while both Cer and S1P treatments further decrease the elasticity of MOSE-L cells. If this is associated with an even more aggressive phenotype and increased tumorigenicity will be addressed in future studies.

Changes in the elastic modulus of MOSE-L cells as a result of the sphingolipid metabolites treatments are shown in Fig. 2. The statistical significance analysis using t-test was assessed. Base on the analysis, Cer and S1P caused a decrease in the average MOSE-L cells elasticity by approximately 15% ($p \approx 0.01$). In contrast, So treatment showed a significant increase in average MOSE-L cells elasticity by 30% ($p \approx 0.0009$).

As shown in Fig. 3, MOSE-L cells exhibit thin and disorganized stress fibers as described previously [16]. Since we have reported previously that actin is a critical determinant of cell viscoelasticity [10, 16], we determined if the changes in the biomechanical properties of cells induced by the treatment with sphingolipid metabolites are associated with an altered actin cytoskeleton organization. Neither Cer nor S1P induced actin stress fibers in MOSE-L cells; in contrast, So-treated MOSE-L cells displayed thicker actin cables and resembled more the less aggressive stages (Fig. 3), confirming earlier results [10] (Creekmore et al., 2012, submitted). This correlates well with the increasing elastic modulus in So-treated MOSE-L cells (Fig. 2). Together, our results suggest that only So can reverse the decreasing elastic modulus in MOSE-L cells while both Cer and S1P make the cells even softer. This may have important ramifications for the design of ovarian cancer treatment strategies using exogenous sphingolipids.

I. Conclusion

The decreasing elasticity and deformability may provide the cancer cells the means for tissue invasion and metastasis. Our studies have identified the critical contributions of the actin cytoskeleton. Here we show that the treatment of aggressive MOSE-L cells with non-toxic concentrations of So, a sphingolipid metabolite that has effectively been used to suppress colon cancer, reversed the elastic modulus of the cells, rendering them stiffer. Sphingolipid metabolites that have been associated with increased cancer growth (S1P) and tumor-promoting inflammation (Cer) did not show the same effects. This suggests that the biomechanical properties of cancer cells are targets of So, and as such may be critical for the suppression of ovarian cancer growth by exogenous So.

References

[1] C. R. Gault, L. M. Obeid, and Y. A. Hannun, "An overview of sphingolipid metabolism: from synthesis to breakdown," Adv Exp Med Biol, vol. 688, pp. 1-23, 2010.

[2] P. Gangoiti, L. Camacho, L. Arana, A. Ouro, M. H. Granado, L. Brizuela, J. Casas, G. Fabrias, J. L. Abad, A. Delgado, and A. Gomez-Munoz, "Control of metabolism and signaling of simple bioactive sphingolipids: Implications in disease," Prog Lipid Res, vol. 49, pp. 316-34, Oct 2010.

[3] E. M. Schmelz, M. C. Sullards, D. L. Dillehay, and A. H. Merrill, Jr., "Colonic cell proliferation and aberrant crypt foci formation are inhibited by dairy glycosphingolipids in 1, 2-dimethylhydrazine-treated CF1 mice," J Nutr, vol. 130, pp. 522-7, Mar 2000.

[4] L. A. Lemonnier, D. L. Dillehay, M. J. Vespremi, J. Abrams, E. Brody, and E. M. Schmelz, "Sphingomyelin in the suppression of colon tumors: prevention versus intervention," Arch Biochem Biophys, vol. 419, pp. 129-38, Nov 15 2003.

[5] L. K. Ryland, T. E. Fox, X. Liu, T. P. Loughran, and M. Kester, "Dysregulation of sphingolipid metabolism in cancer," Cancer Biol Ther, vol. 11, pp. 138-49, Jan 15 2011.

[6] G. M. Strub, M. Maceyka, N. C. Hait, S. Milstien, and S. Spiegel, "Extracellular and intracellular actions of sphingosine-1-phosphate," Adv Exp Med Biol, vol. 688, pp. 141-55, 2010.

[7] A. N. Hanna, L. G. Berthiaume, Y. Kikuchi, D. Begg, S. Bourgoin, and D. N. Brindley, "Tumor necrosis factor-alpha induces stress fiber formation through ceramide production: role of sphingosine kinase," Mol Biol Cell, vol. 12, pp. 3618-30, Nov 2001.

[8] P. A. Singleton, S. M. Dudek, E. T. Chiang, and J. G. Garcia, "Regulation of sphingosine 1-phosphate-induced endothelial cytoskeletal rearrangement and barrier enhancement by S1P1 receptor, PI3 kinase, Tiam1/Rac1, and alpha-actinin," FASEB J, vol. 19, pp. 1646-56, Oct 2005.

[9] P. C. Roberts, E. Motillo, A. C. Baxa, H. H. Q. Heng, N. Doyon-Reale, L. Gregoire, W. D. Lancaster, R. Rabah, and E. M. Schmelz, "Sequential Molecular and Cellular Events during Neoplastic progression: A Mouse Syngeneic Ovarian Cancer Model," Neoplasia, vol. 7, pp. 944-956, 2005.

[10] A. L. Creekmore, W. T. Silkworth, D. Cimini, R. V. Jensen, P. C. Roberts, and E. M. Schmelz, "Changes in Gene Expression and Cellular Architecture in an Ovarian Cancer Progression Model," PLoS ONE, vol. 6, p. e17676.

[11] A. N. Ketene, E. M. Schmelz, P. C. Roberts, and M. Agah, "The effects of cancer progression on the viscoelasticity of ovarian cell cytoskeleton structures," Nanomedicine : nanotechnology, biology, and medicine, vol. 8, pp. 93-102.

[12] E. C. Faria, N. Ma, E. Gazi, P. Gardner, M. Brown, N. W. Clarke, and R. D. Snook, "Measurement of elastic properties of prostate cancer cells using AFM," Analyst, vol. 133, pp. 1498-1500, 2008.

[13] S. E. Cross, Y.-S. Jin, J. Rao, and J. K. Gimzewski, "Nanomechanical analysis of cells from cancer patients," Nat Nano, vol. 2, pp. 780-783, 2007.

[14] Q. S. Li, G. Y. H. Lee, C. N. Ong, and C. T. Lim, "AFM indentation study of breast cancer cells," Biochemical and Biophysical Research Communications, vol. 374, pp. 609-613, 2008.

[15] M. Nikkhah, J. S. Strobl, E. M. Schmelz, and M. Agah, "Evaluation of the influence of growth medium composition on cell elasticity," Journal of Biomechanics, vol. 44, pp. 762-766.

[16] A. N. Ketene, P. C. Roberts, A. S. Shea, E. M. Schmelz, and M. Agah, "Actin filaments play a primary role for structural integrity and viscoelastic response in cells," Integrative Biology, 2012.

[17] E. K. Dimitriadis, F. Horkay, J. Maresca, B. Kachar, and R. S. Chadwick, "Determination of Elastic Moduli of Thin Layers of Soft Material Using the Atomic Force Microscope," Biophysical journal, vol. 82, pp. 2798-2810, 2002.

[18] A. Vinckier and G. Semenza, "Measuring elasticity of biological materials by atomic force microscopy," FEBS Letters, vol. 430, pp. 12-16, 1998.

[19] P. Carl and H. Schillers, "Elasticity measurement of living cells with an atomic force microscope: data acquisition and processing," Pflugers Arch., vol. 457, pp. 551-559, 2008.